NSTX-U

Supported by U.S. DEPARTMENT OF ENERGY Office of Science

Experimental Study of Kink-like Modes in NSTX Plasmas

College W&M
Colorado Sch Mines
Columbia U
CompX
General Atomics
INEL
Johns Hopkins U
LANL
LLNL
Lodestar
MIT
Nova Photonics
New York U
Old Dominion U
ORNL
PPPL
PSI
Princeton U
Purdue U
SNL
Think Tank, Inc.
UC Davis
UC Irvine
UCLA
UCSD
U Colorado
U Illinois
U Maryland
U Rochester
U Washington
U Wisconsin

Ge Dong and Mario Podesta
Princeton Plasma Physics Lab
and the NSTX-U Research Team

APS-DPP
New Orleans, Louisiana
October, 2014

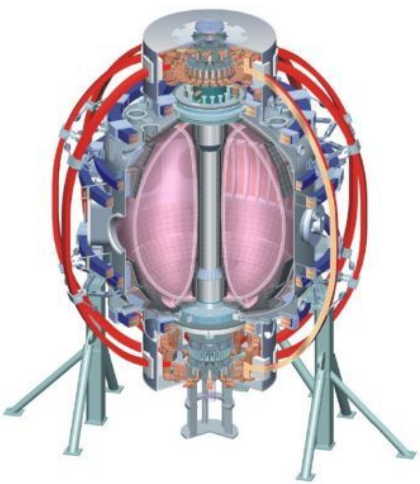

Culham Sci Ctr
U St. Andrews
York U
Chubu U
Fukui U
Hiroshima U
Hyogo U
Kyoto U
Kyushu U
Kyushu Tokai U
NIFS
Niigata U
U Tokyo
JAEA
Hebrew U
Ioffe Inst
RRC Kurchatov Inst
TRINITI
KBSI
KAIST
POSTECH
ASIPP
ENEA, Frascati
CEA, Cadarache
IPP, Jülich
IPP, Garching
ASCR, Czech Rep
U Quebec

Introduction

Wave number spectrum from the Mirnov coils

Effective mode growth rate and real frequency

Stability trend with thermal plasma and fast ion parameters

Conclusions and Future work

Outline

- Introduction
  - Motivations
  - National Spherical Torus Experiment (NSTX) plasma properties in the kink-like mode studies
- Non-resonant kink (NRK) and fishbone dynamics
  - Wave number spectrum from the Mirnov coils
  - Effective mode growth rate and real frequency
  - Relationship with thermal plasma and fast ion parameters
- Conclusions and future work

Introduction- Motivation

- Internal Kink modes destabilized by energetic particles can cause particle losses and deteriorate plasma performance in toroidal fusion devices.
- NSTX primarily uses neutral beam injection (NBI) for heating and current drive, thus introducing a large super-Alfvenic fast ion population into the plasma[3]. The precessional[4] and bounce[5] resonance of the fast ions with internal kink-like modes[6] provides drive for the fishbone modes, and the consequential fast ion transport can significantly affect plasma β (= $8\pi nT/B^2$).
- Detailed characterization of the kink-like instabilities in NSTX plasmas can provide reference for validation and benchmark for theoretical[9] and numerical[10],[11] studies.

Introduction- NSTX plasma properties

- B_T ~ 0.4 T, n_e~ 3 × $10^{19}m^{-3}$, T_e ~ T_i ~ 1.5keV . The flux surfaces are re-construced using LRDFIT, constrained by Thomson Scattering (TS), charge-exchange recombination spectroscopy (CHERS) and MSE measurements.

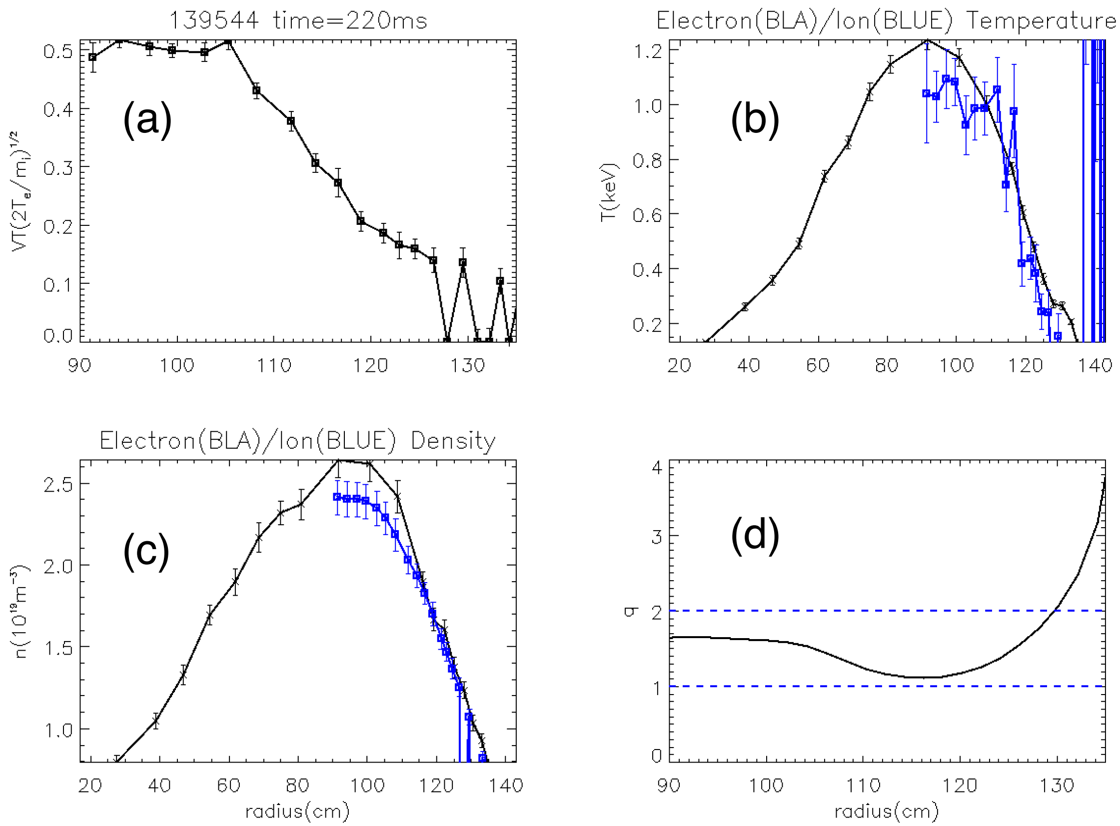

•Experimental rotation (a), temperature (b), density (c) and q (d) profile for shot # 139544 at 200 ms.

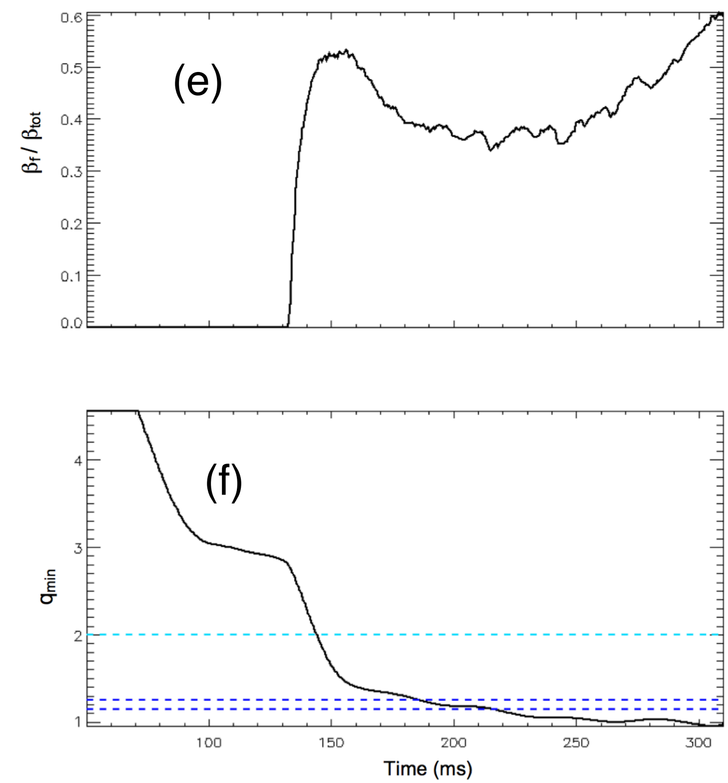

•Time evolution of β_f (e) and minimum q (f) from TRANSP simulation results for shot # 139544.

Transition from fishbones to Non-Resonant Kink (NRK) are observed in shots with different P_{NB}

- Fishbone and NRK are analyzed in shots with different scenarios and NB power. Transitions from fishbones to NRK are observed.

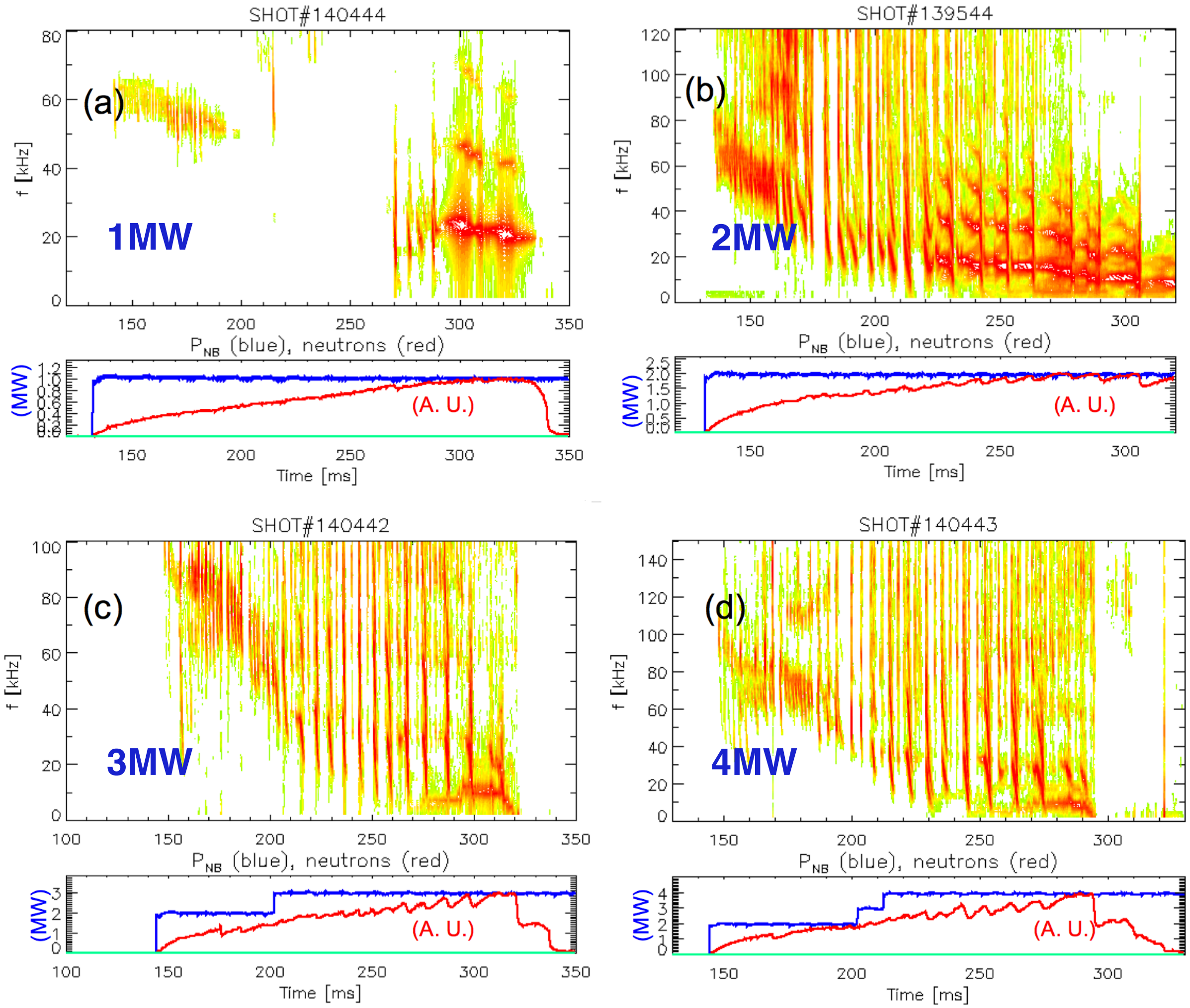

•Spectrograms of magnetic fluctuations in shot # 140444 (a), 139544(b), 140442(c) and 140443(d), with NB power 1MW, 2MW, 3MW and 4MW, respectively.

Bursting modes correlate with large fast ion transport events, as deduced by drops in neutron rate

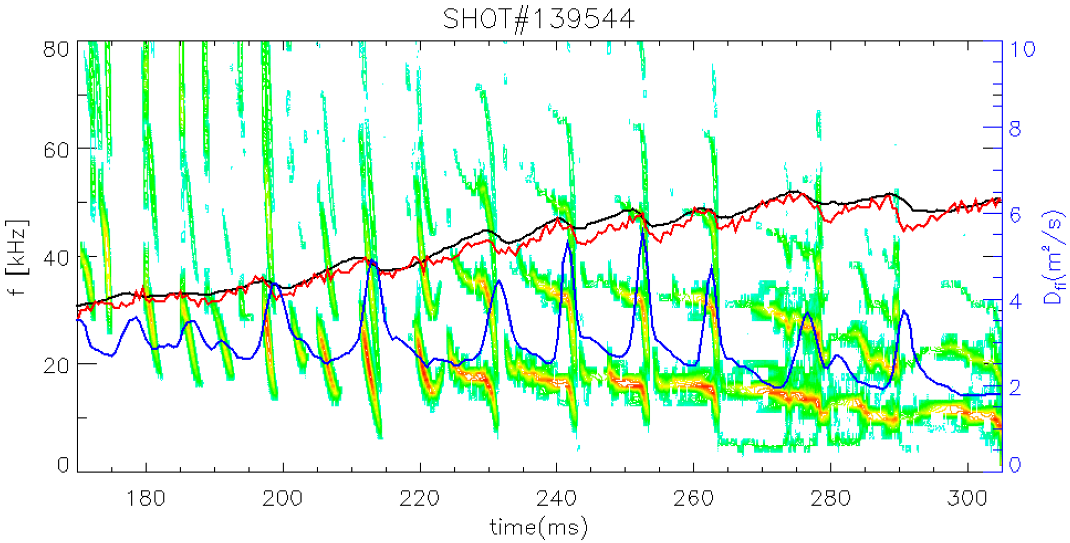

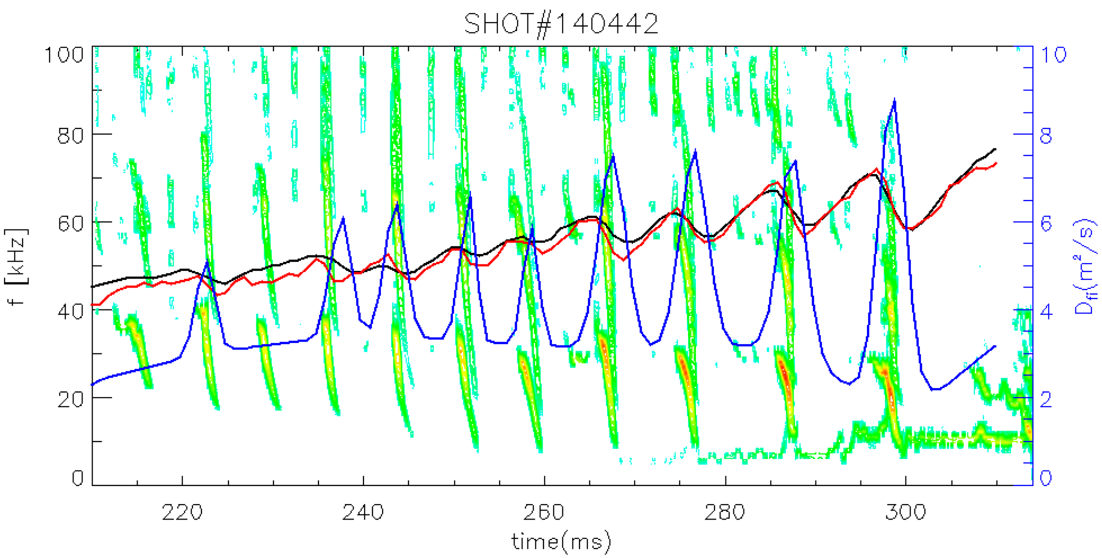

- The fast ion dynamics is simulated using TRANSP, with imposed fast ion diffusivity to match the measured neutron rates.
- Fishbone bursts correspond to large fast ion transport events, with measured neutron rate drops up to around 50%.

Imposed diffusivity

Measured neutron rate

Simulated neutron rate

•TRANSP simulation results and spectrogram for shot # 139544 and140442

Fast ion transport has an increasing trend with the bursting mode amplitude

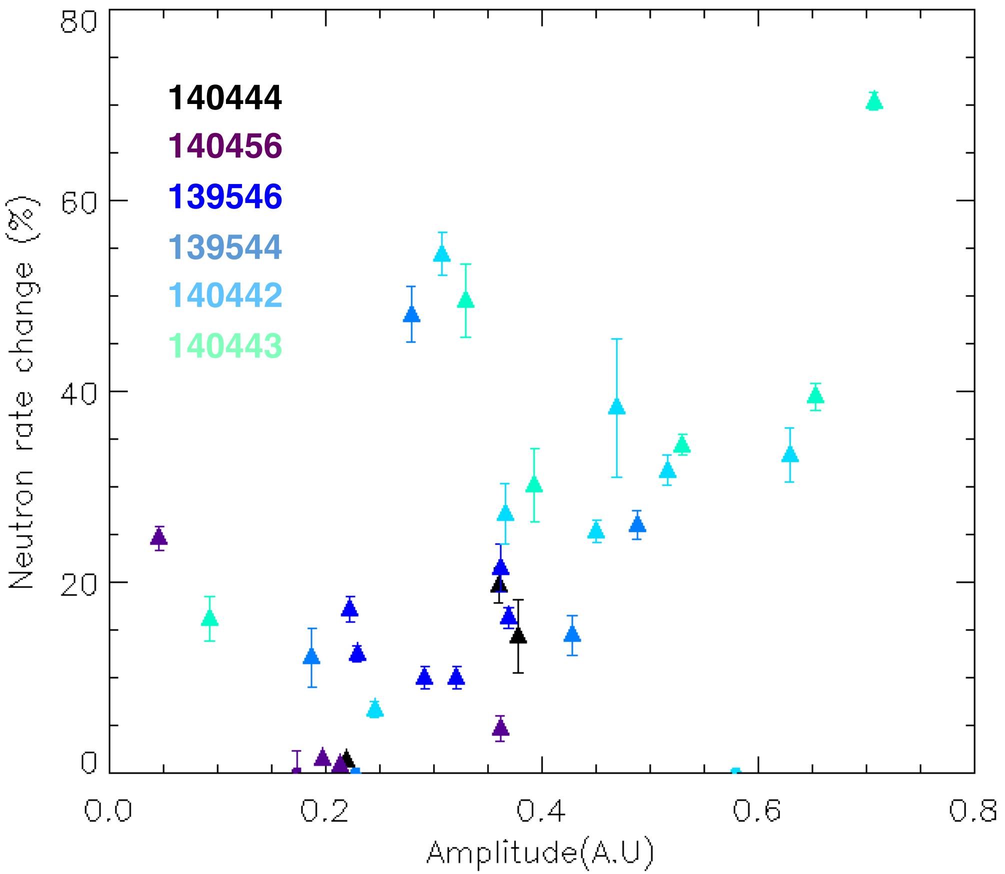

•Relationship between neutron rate change and mode amplitude for bursting events. Colors represent different shots.

• The bursting modes amplitude is measured from the Mirnov coil signals.

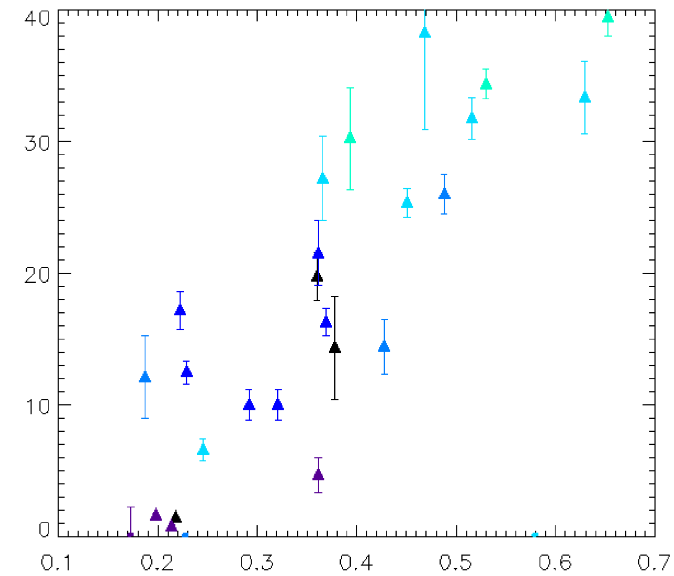

•Cropped figure for neutron rate decrease from 0-40 percent, and for mode amplitude from 0.1-0.7.

- The neutron rate decreases correlates well with the mode amplitudes, especially for the central range of both parameter (cropped figure).
- This implies that the fast ion transport rate might has a strong dependence on mode amplitude.

Bursting modes and long-lived modes are identified as fishbones and NRKs

- The bursting modes with lifetime~2 ms and chirping frequency δ *f* ~ 10 kHz are identified as fishbone oscillations (a). The long-lived modes with lifetime ≥ 10 ms appearing near the end of the discharges are identified as kink modes (b).

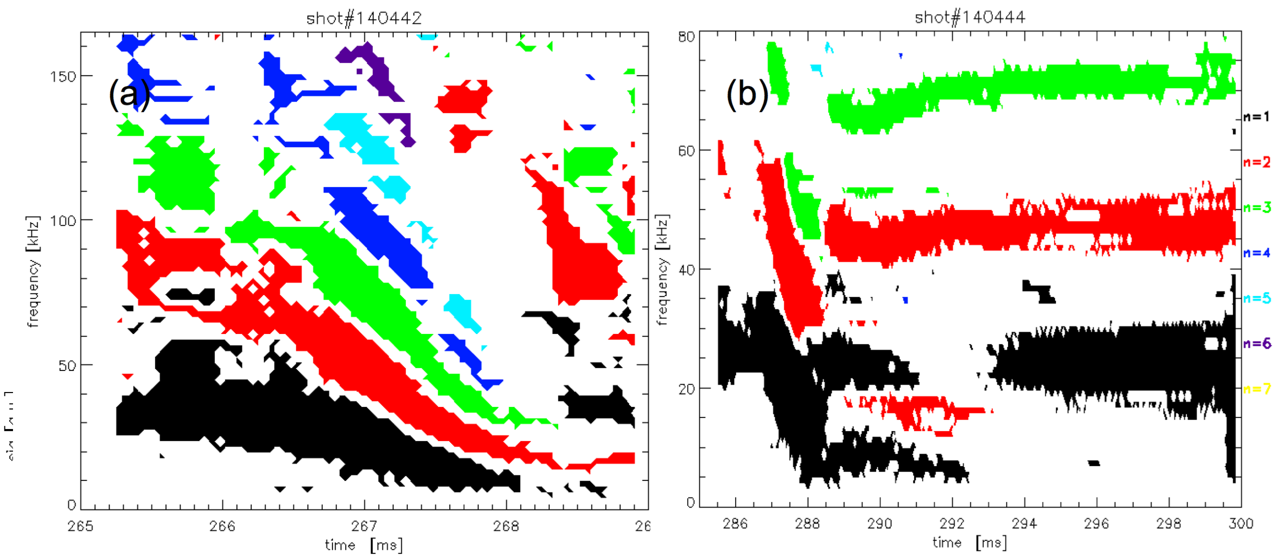

• Spectrogram of Mirnov coil signal with toroidal mode number during ~ 267 ms in shot # 140442 (a), and during ~ 295 ms in shot # 140444 (b)

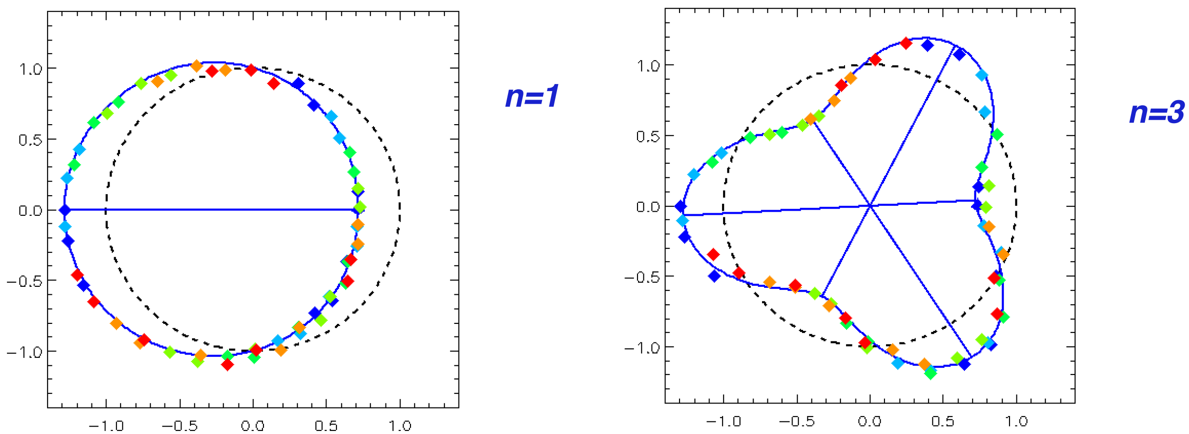

•Polar plot of the mode amplitude versus coil sensor toroidal angle fitted with a sinusoid. Data refer to the n =1, 3 fishbone harmonic at t = 267 ms in shot # 140442.

Details in fishbone frequency chirping

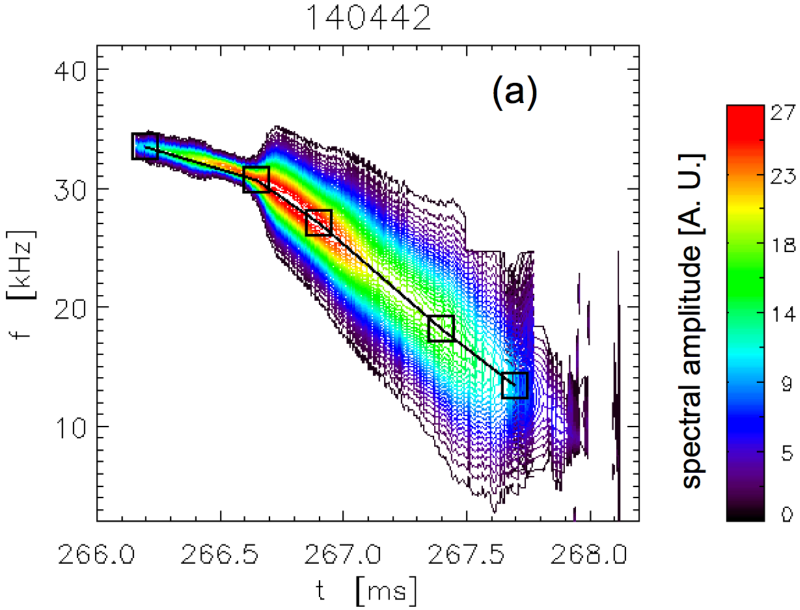

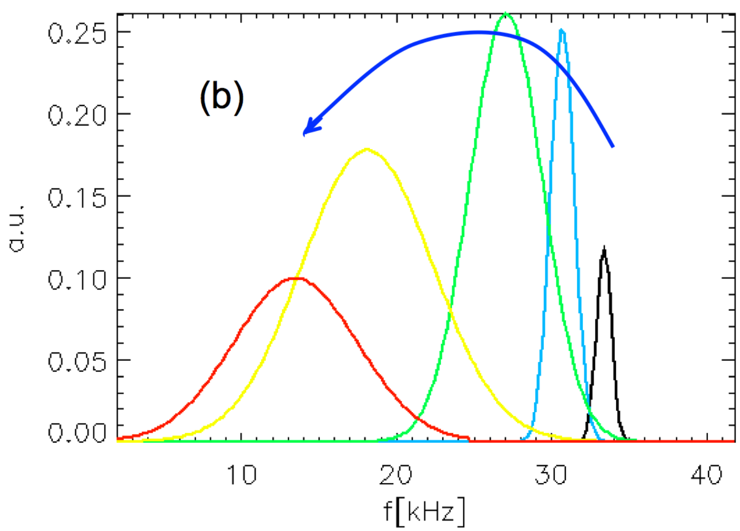

- The fishbone modes generally have a chirping frequency from ~ 30 kHz to ~ 15 kHz in the lab frame for the dominant n=1, m=1 harmonic.
- The spectrum also become broader as the frequency drops (b). This pattern repeats itself with a interval also on the time scale of ~5 ms.

•Details of the n=1 harmonic in the chirping fishbone mode. The black squares in (a) indicate time points where the spectrum is plotted in (b).

Effective mode growth rate and real frequency

- The frequency separations between peaks with consecutive n's are almost constant, for both fishbones and NRKs, implying different harmonics of the mode have a same real frequency on top of the Doppler shift caused by toroidal rotation[3], i. e.

$$f_{lab,n}^{mode} = f_r^{mode} + n\, f_{Doppler}$$

- Linear fit can be done for the instability events in the spectrum time evolution to extract f_r^{mode} and $f_{Doppler}$.
- Effective growthrate is calculated by exponential fit to the mode amplitude evolution

Real frequency and effective growthrate evolution are distinctive of each type of instability (fishbone, NRK)

- **Time evolution of various parameters during one fishbone(a) and kink (b) event.**

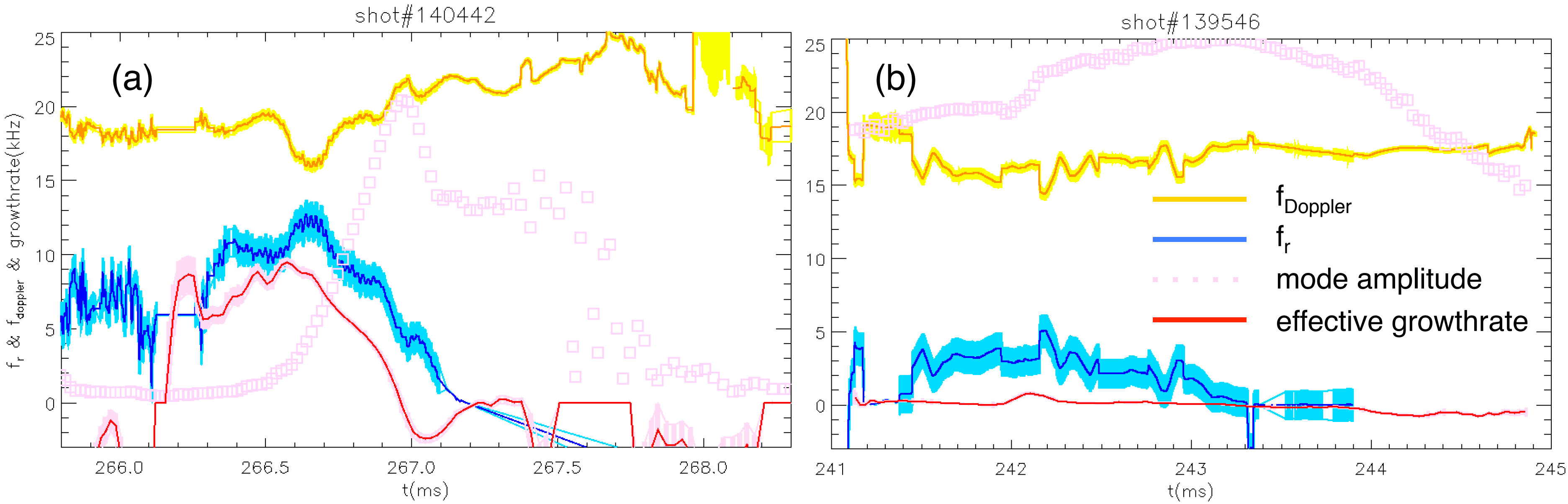

•For the fishbone mode, the real frequency drops from ~ 15 kHz to 0, indicating a strong interaction with the fast ions.

•For the NRK mode, the real frequency stays almost 0, implying its ideal MHD nature. The Doppler shift frequency is of the same order of magnitude at ~ 18 kHz.

•The shadow area indicate error bars for the linear fit.

Real frequency decreases for lower P_{NB} shots as the NRK regime is approached

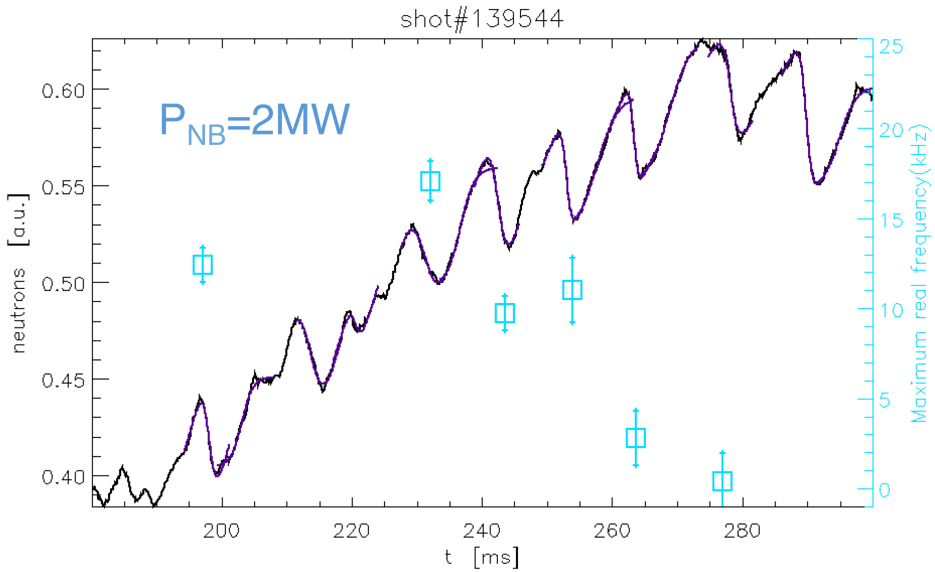

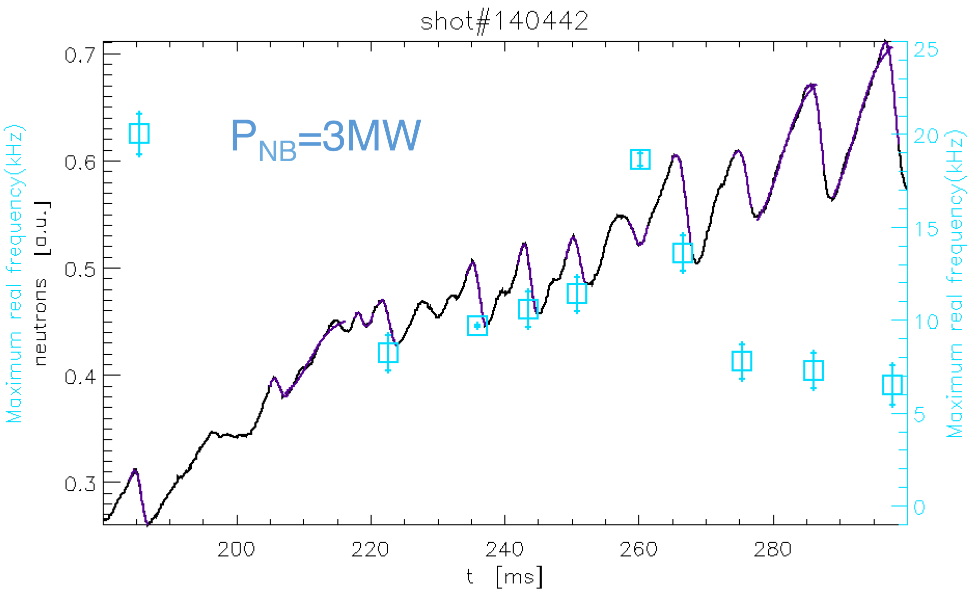

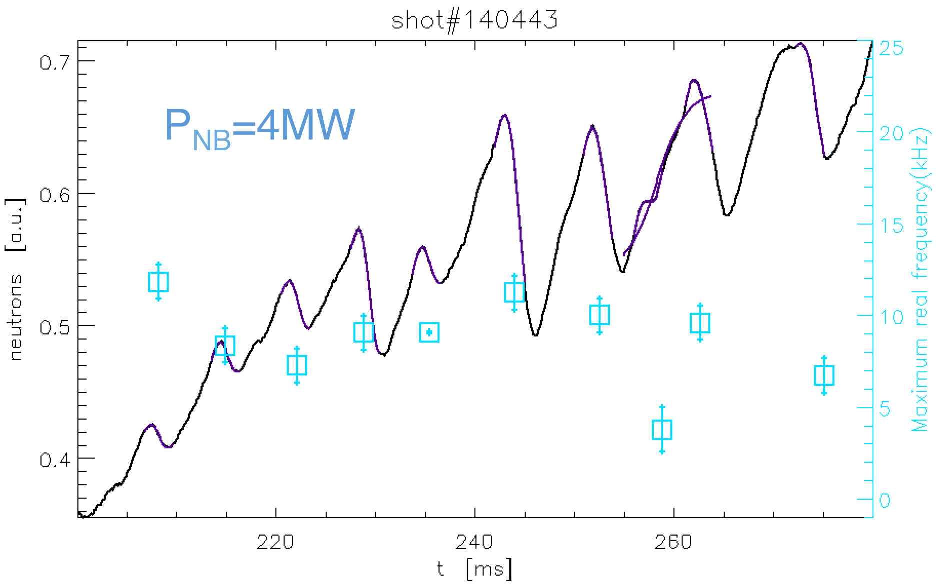

- For each bursting fishbone event, this analysis gives a maximum mode real frequency and growthrate.
- For lower NB power shots, the mode real frequency decreases as the plasma is closer to NRK regime .

Effective mode growthrate decreases for lower and higher P_{NB} shots as the NRK regime is approached

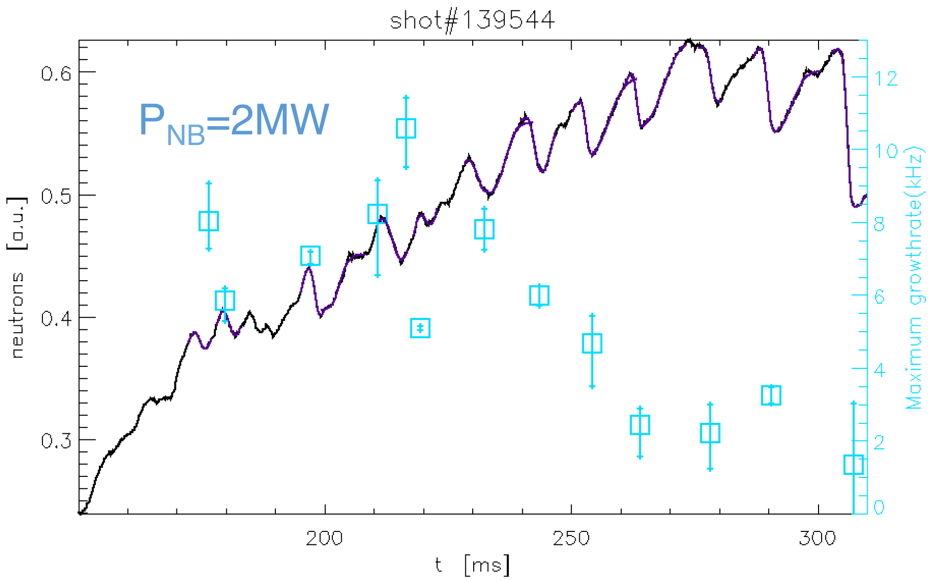

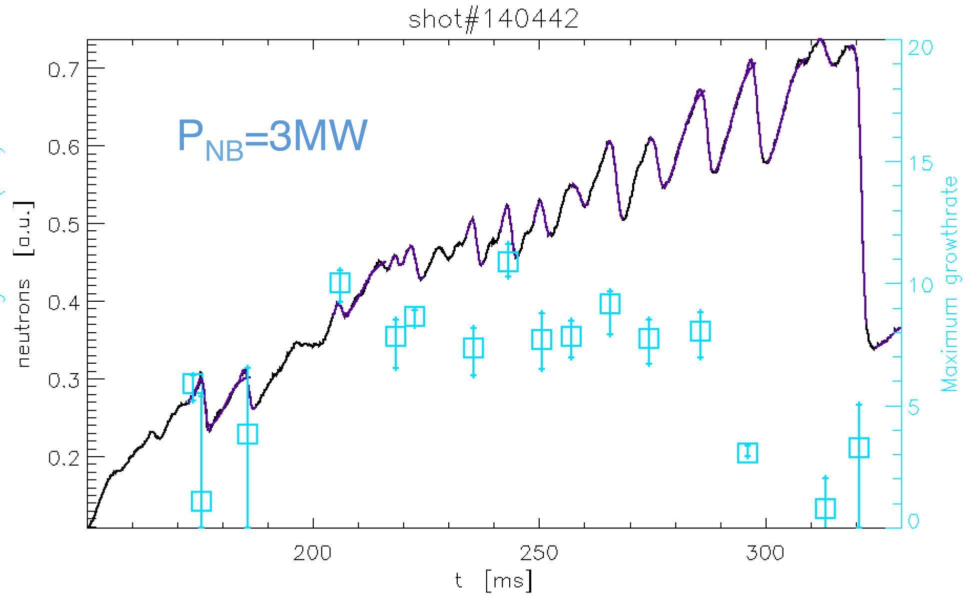

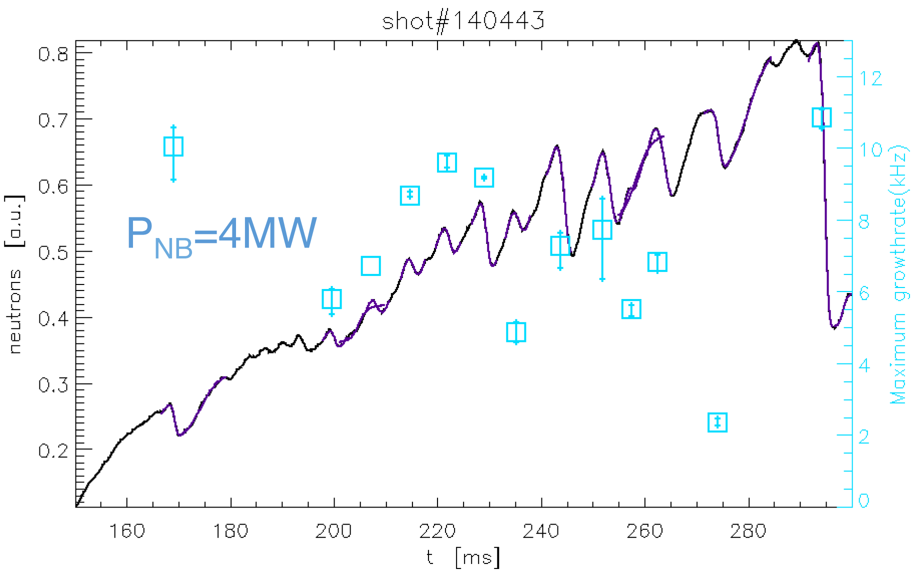

- The maximum growthrate exhibits a decreasing trend towards the NRK regime for the discharges with NB power from 2-4 MW.

Kink-like modes are unstable below q_{min} ~1.5

Trends of fishbone and kink stability with selected parameters (e.g. β, q_{min}) can be found from this database.

Fishbone and NRK stability diagram in β_{beam}/β_{tot} -q_{min} space

- **Blue dots represent fishbone events**
- **Red dots represent NRK events**
- **Black circles represent no instability below 40kHz.**
- **Light blue crosses represent mode transition from fishbone to NRK in different shots**

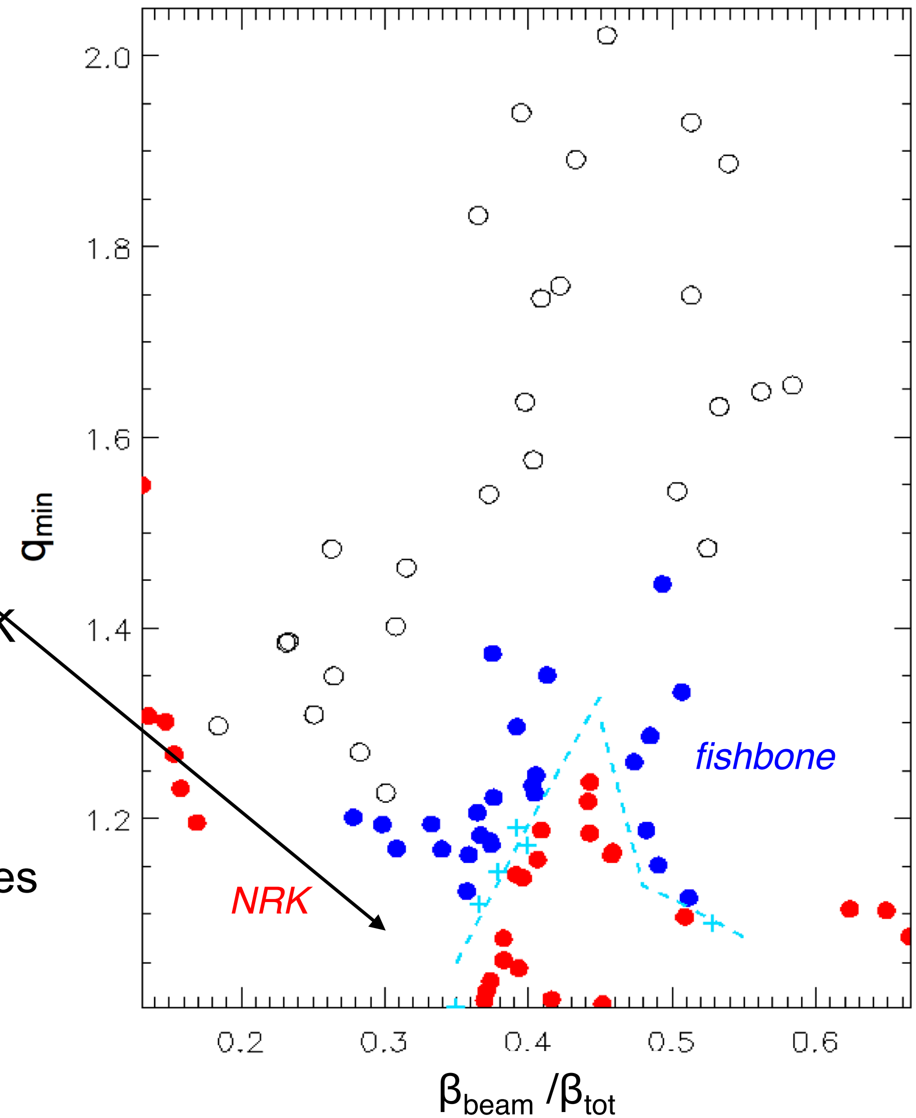

- The mode could be marginal between NRK and fishbone near the transition point.
- Above q_{min} = 1.55, no mode is observed.
- NRKs appear at low β_{beam}/β_{tot} values.
- The regime around β_{beam}/β_{tot} ~ 0.4 becomes most NRK unstable.
- The fishbone events become unstable at β_{beam}/β_{tot} ~ 0.25.

Stability diagram in different parameter spaces indicate fishbone and NRK dependence on β_{beam}

Fishbone and kink activity diagrams in different quantity space

Colored lines in (a) represent time history of q_{min} and β_{beam}/β_{tot} in different shots

(a) The time evolutions of the two quantities in various shots do not have a clear trend, indicating no hidden dependence of the mode stabilities on time.

(b) The NRK is mostly unstable at higher β_{beam} and lower q_{min}, and the fishbones are mostly unstable at lower β_{beam} an higher q_{min} in the parameter regime the data base scans

(c) The instabilities depend on β_{tot} weakly

(d) T_e and n_e range is ~(1,1.4)keV and $(1,4)10^{19}m^{-3}$, repectively

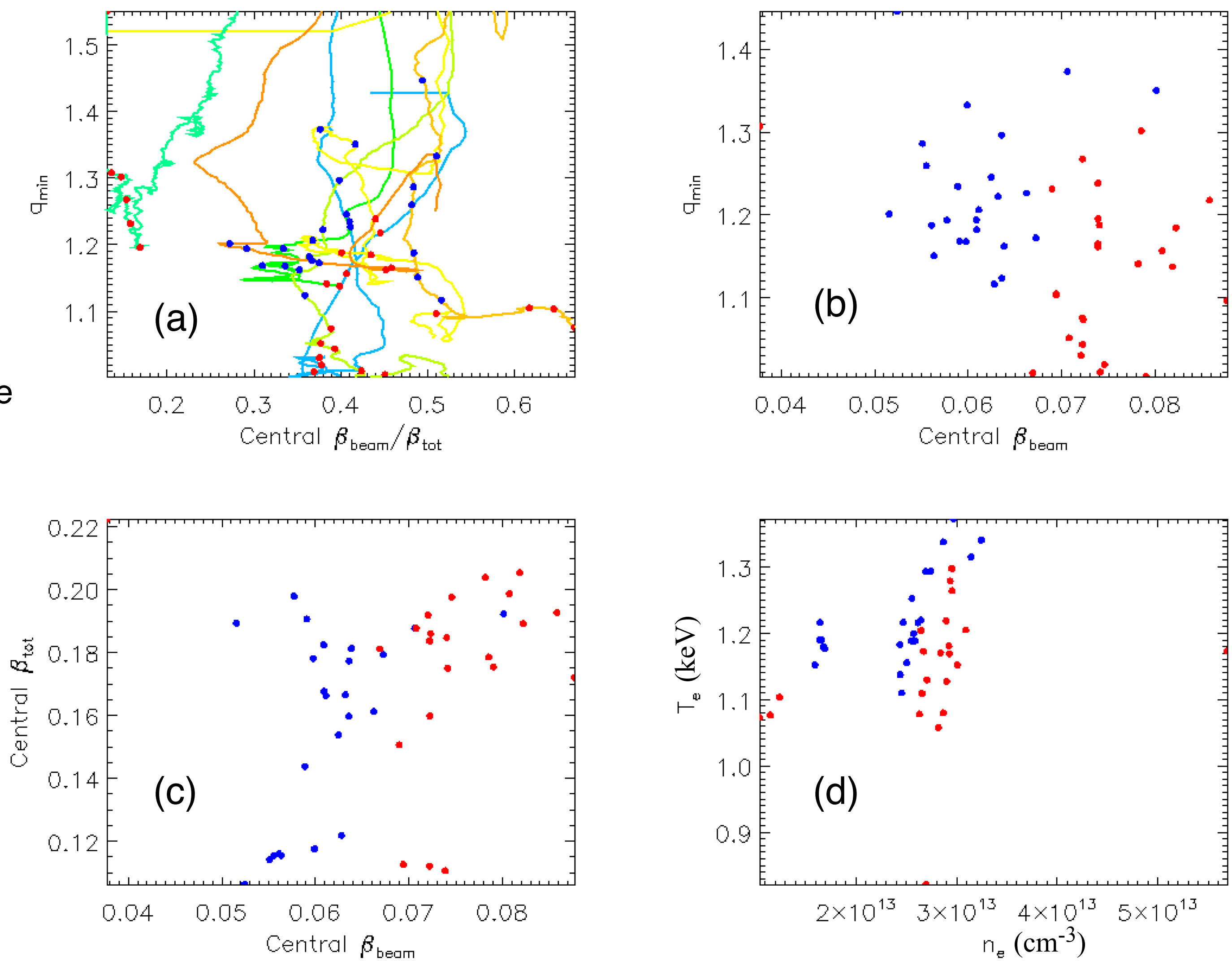

Bursting mode real frequency has increasing trend with β_{beam}/β_{tot} and q_{min}

Fishbone and marginal bursting mode stability diagram with mode frequency change

Size and color of the events represent the maximum real frequency

The mode real frequency increases with β_{beam}/β_{tot} and q_{min}

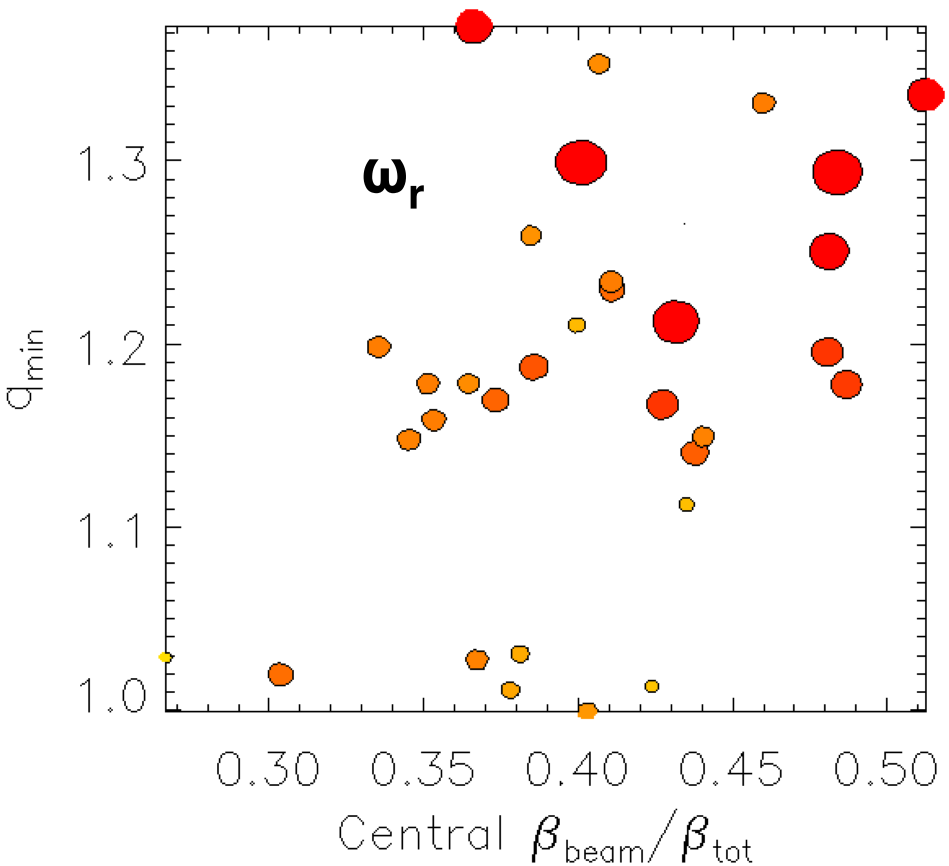

The mode real frequency depends weakly on β_{beam}

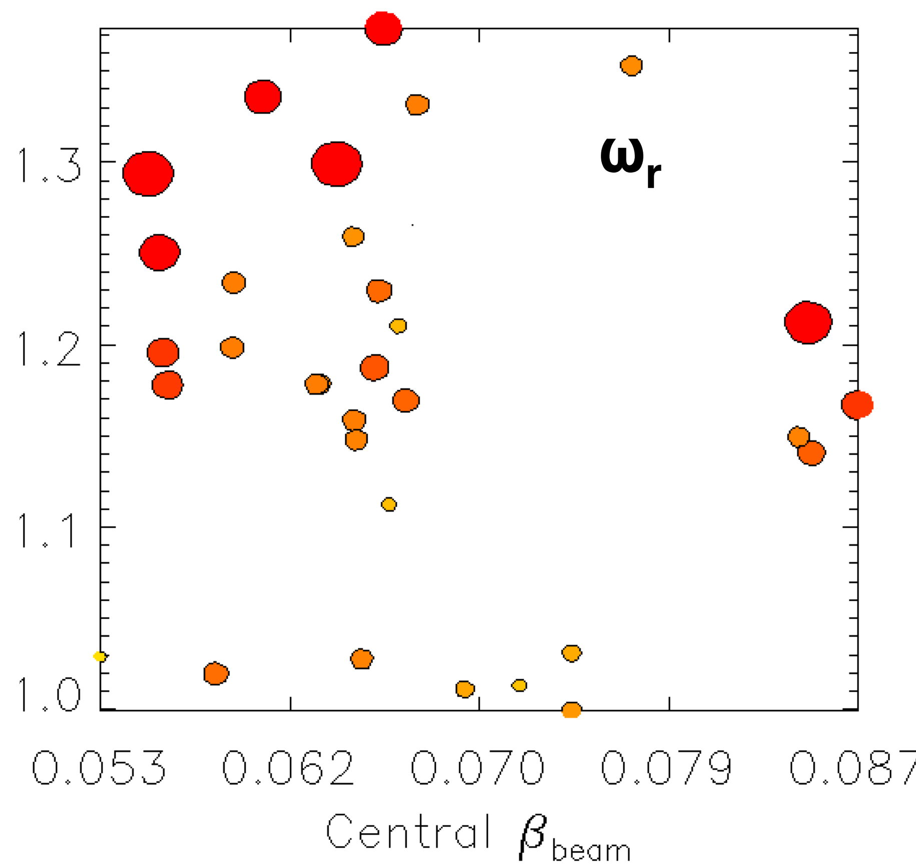

Mode amplitude has decreasing trend with β_{beam}/β_{tot} and q_{min} Effective growthrate depends weakly on either parameter

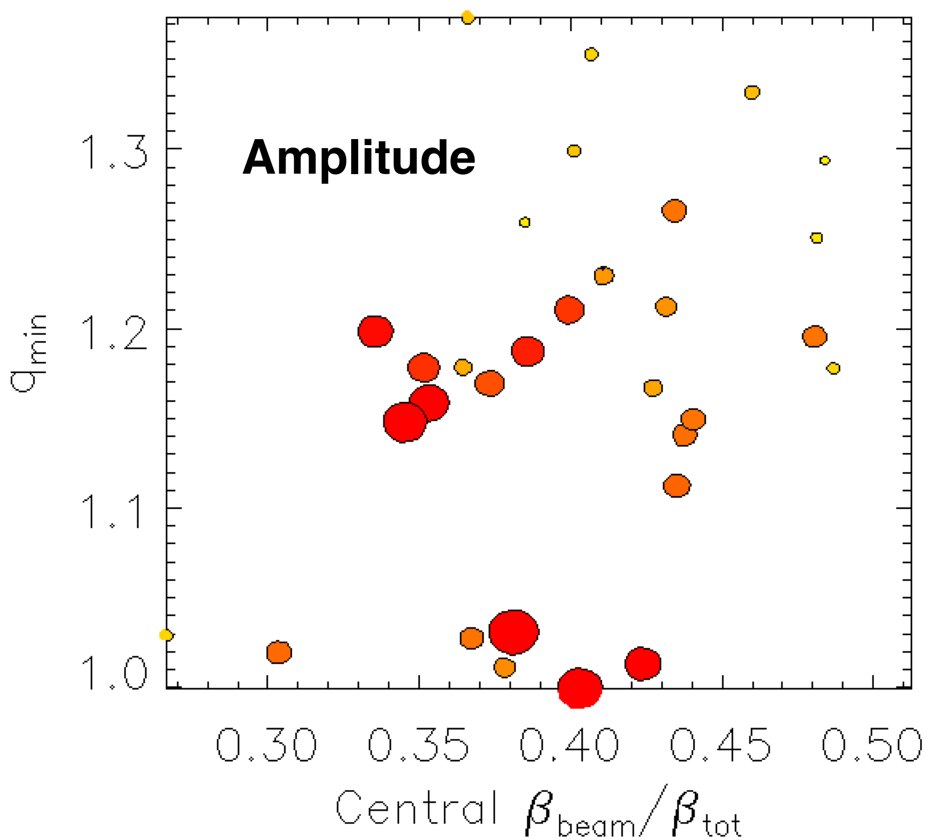

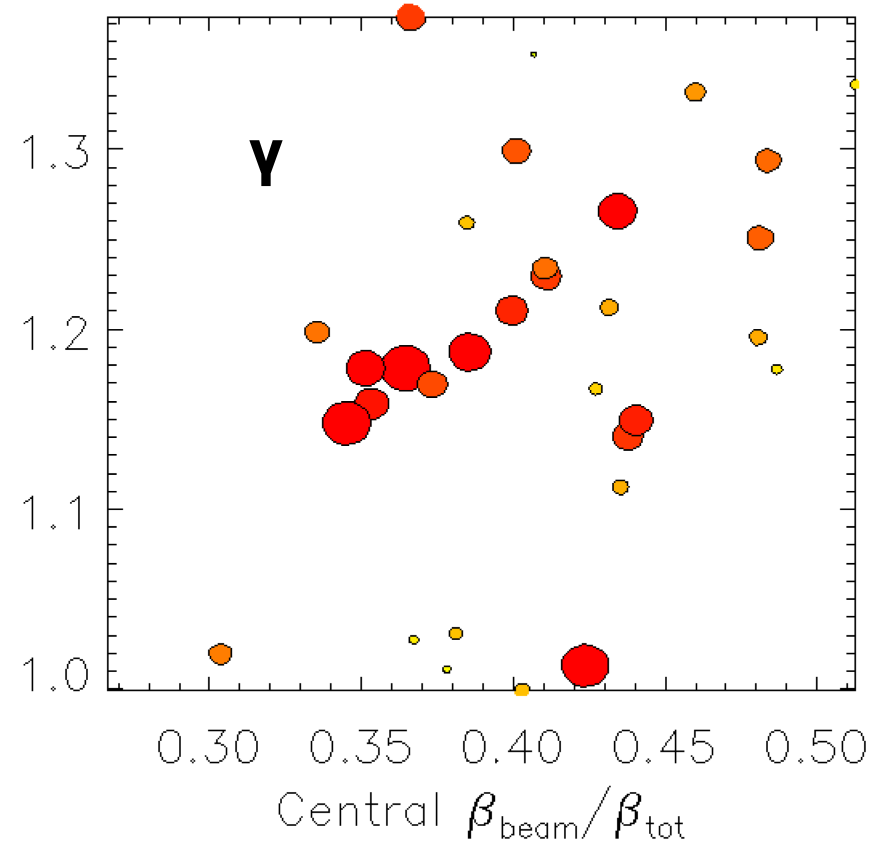

- Stability diagram with mode amplitude change indicates the mode amplitude decreases with β_{beam}/β_{tot} and q_{min}
- Stability diagram with effective growth rate shows no clear trend with β_{beam}/β_{tot} and q_{min}

Dependence of mode properties on resonant fast ion parameters

- Since the dependence of mode properties shows only weak trends on global parameters, fast ions satisfying the precessional resonance condition $\omega_r = n\,\omega_{pre}$ are selected. Where n=1 is the dominant toroidal mode number for kink-like modes.
- The resonant fast ion β: $\beta_{res}=\beta_{beam}$ integrated along the $\omega_r = \omega_{pre}$ line in the phase space to select resonant fast ions, where $\omega_r = 2\pi f_r$, and ω_{pre} is the fast ion precessional frequency given by[15]

$$\omega_{pre} = \frac{2E}{R_0 B_0}\frac{q}{r}(2-\lambda)\left[\frac{\mathbf{E}(k)}{\mathbf{K}(k)} - \frac{1}{2} + \left(\frac{\mathbf{E}(k)}{\mathbf{K}(k)} + k - 1\right)\right]$$

  - E is the fast ion energy.
  - E(k) and K(k) are the complete elliptic functions
  - $k = (1 + \varepsilon - \lambda)/2\varepsilon$
  - $\varepsilon = r/R_0$
  - $\lambda = \mu B_0/E$ is a velocity space variable related to pitch angle.

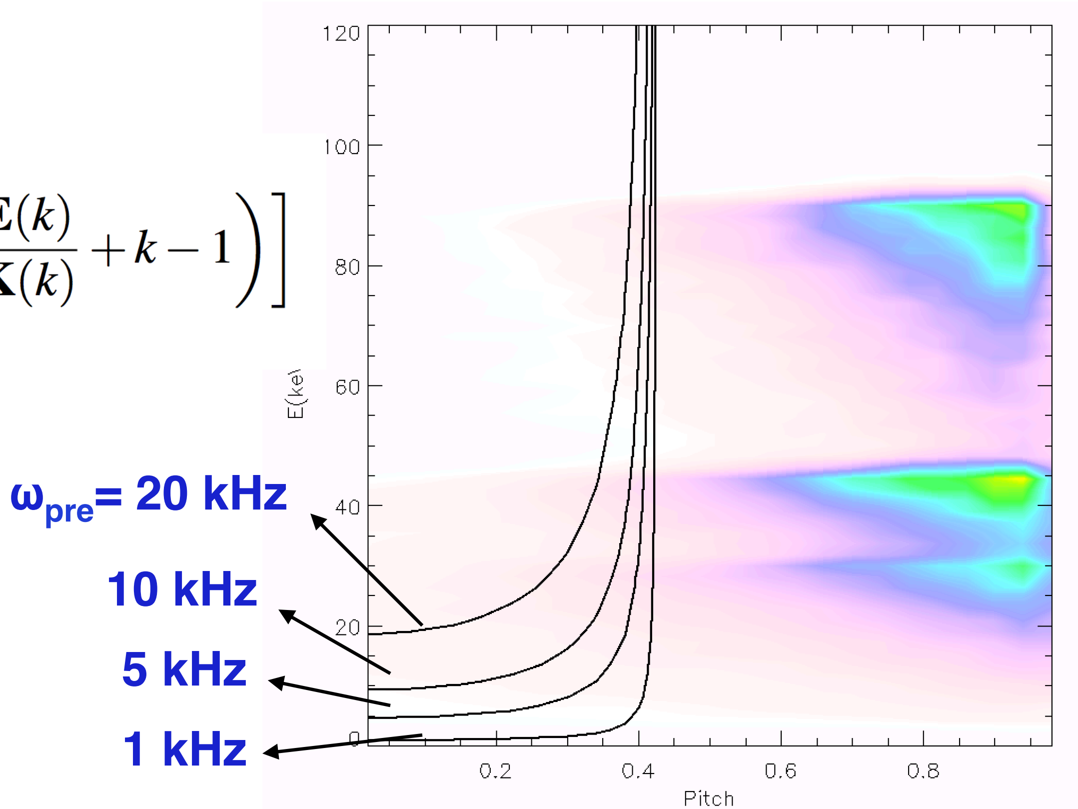

Fast ion phase space distribution from TRANSP

Growthrate exhibits a general increasing trend with β_{res}

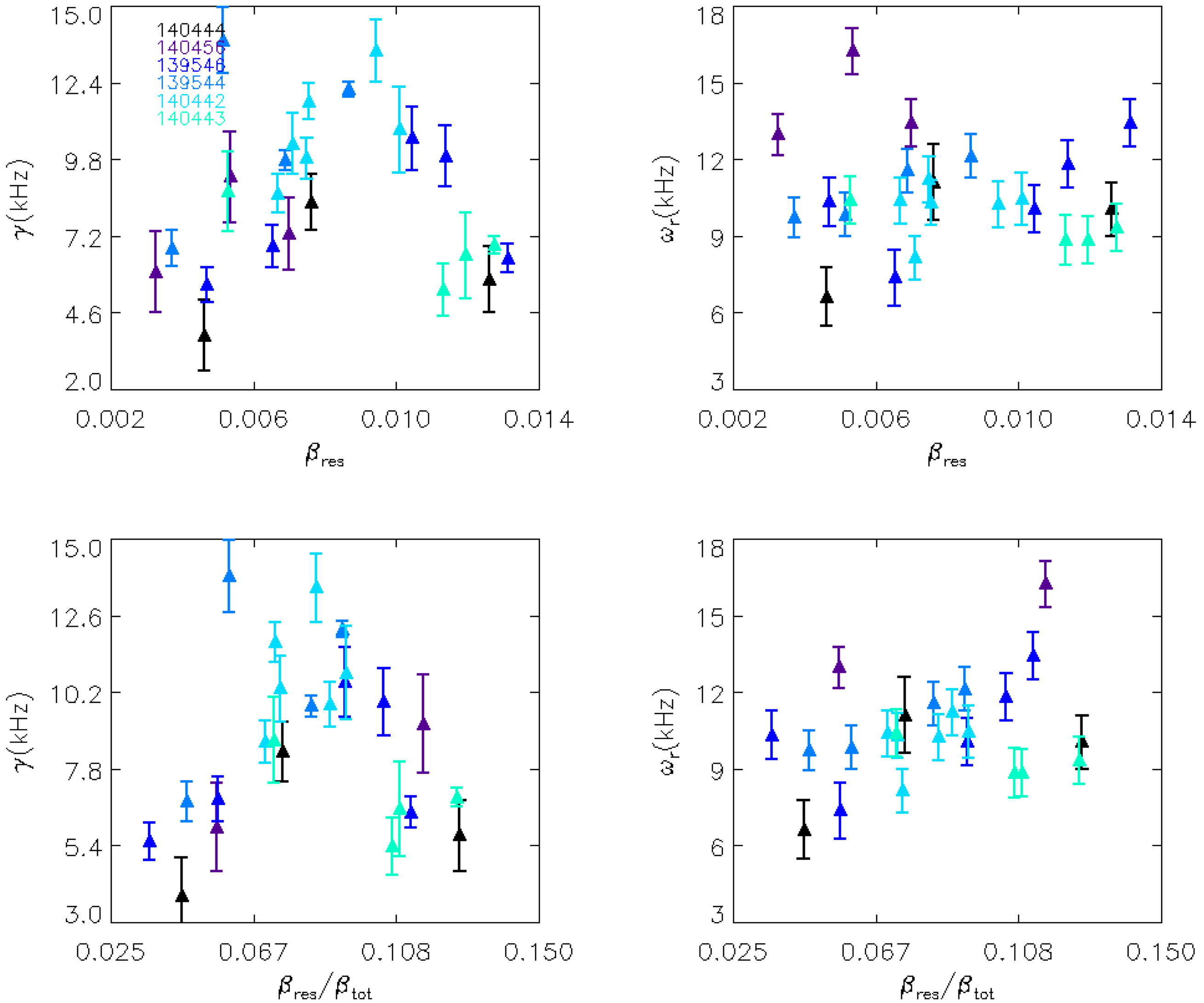

- β_{res} is the integrated fast ion β along the $\omega_r = \omega_{pre}$ line in the phase space.
- The growthrate has a increase trend with resonant β_{res}
- except for a drop at higher β_{res}, corresponding to $\beta_{res} / \beta_{tot} \sim 0.3$.

ORBIT code reveals multiple resonances are at play in addition to "precession" resonance

- Resonances identified through "phase vector rotation" method in ORBIT [White, PPCF **53** 085018 2011]
- Consistent with previous studies of *bounce-precession fishbones* in NSTX [Fredrickson, NF **43** 1258 2003]

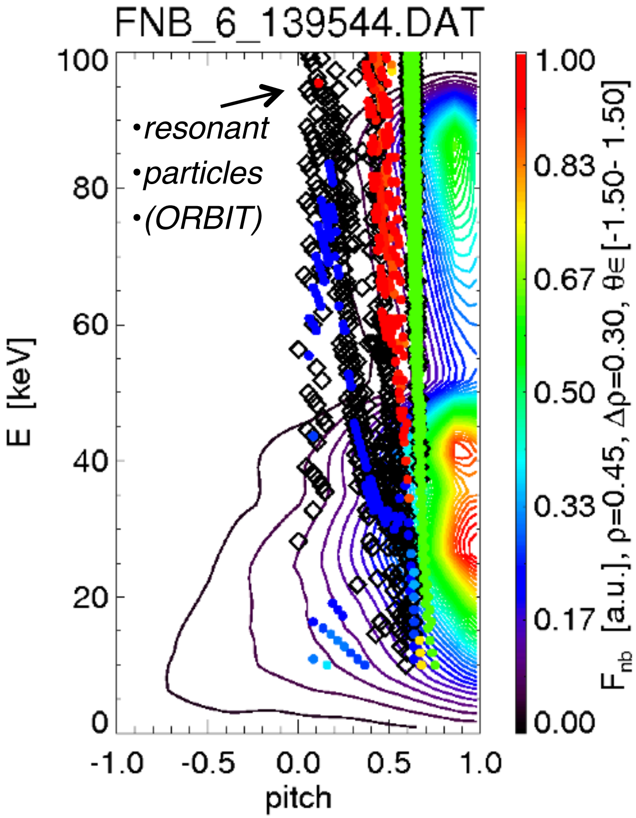

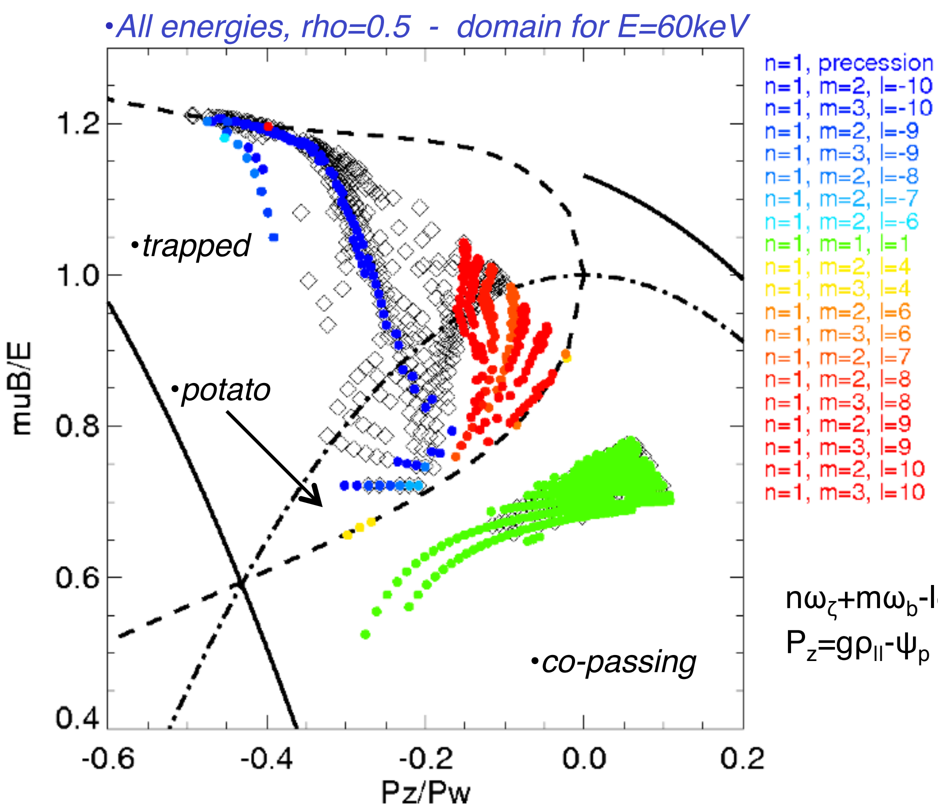

$n\omega_\zeta + m\omega_b - l\omega_n = 0$

$P_z = g\rho_{||} - \psi_p$

Poincaré plots show signature of resonances over broad portion of trapped/co-passing phase space

Points are plotted in the poloidal cross section whenever $n\zeta-\omega_n t=2\pi k$

E=90keV, $\mu B_0/E$~1

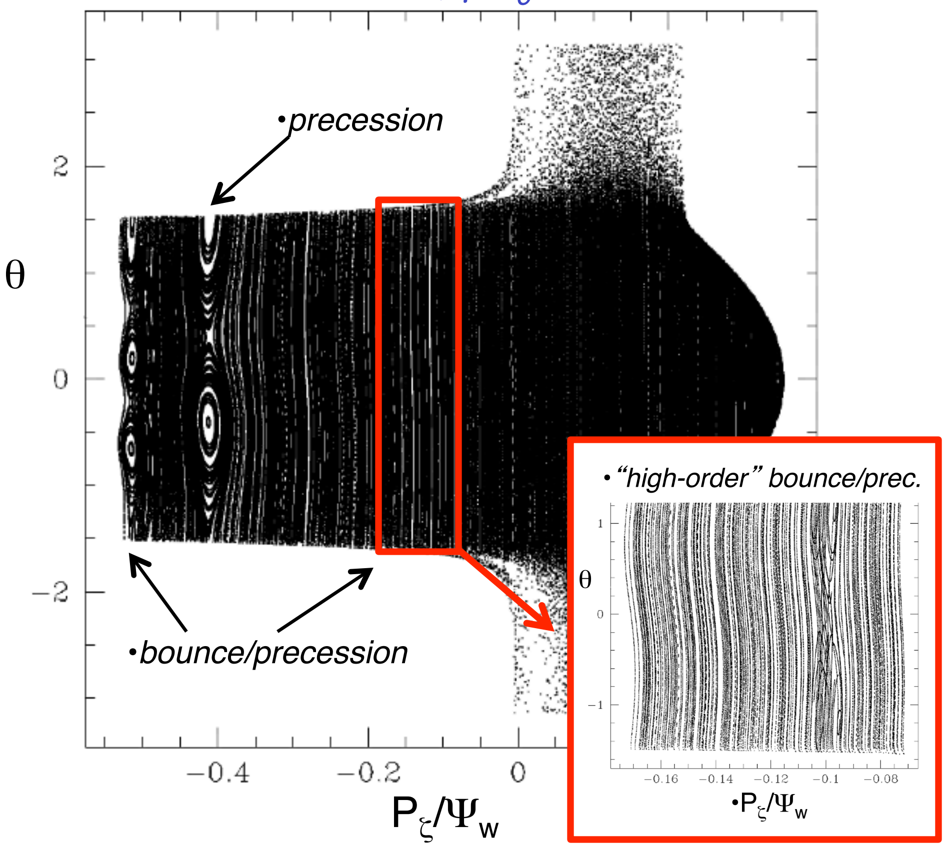

E=90keV, $\mu B_0/E$~0.3

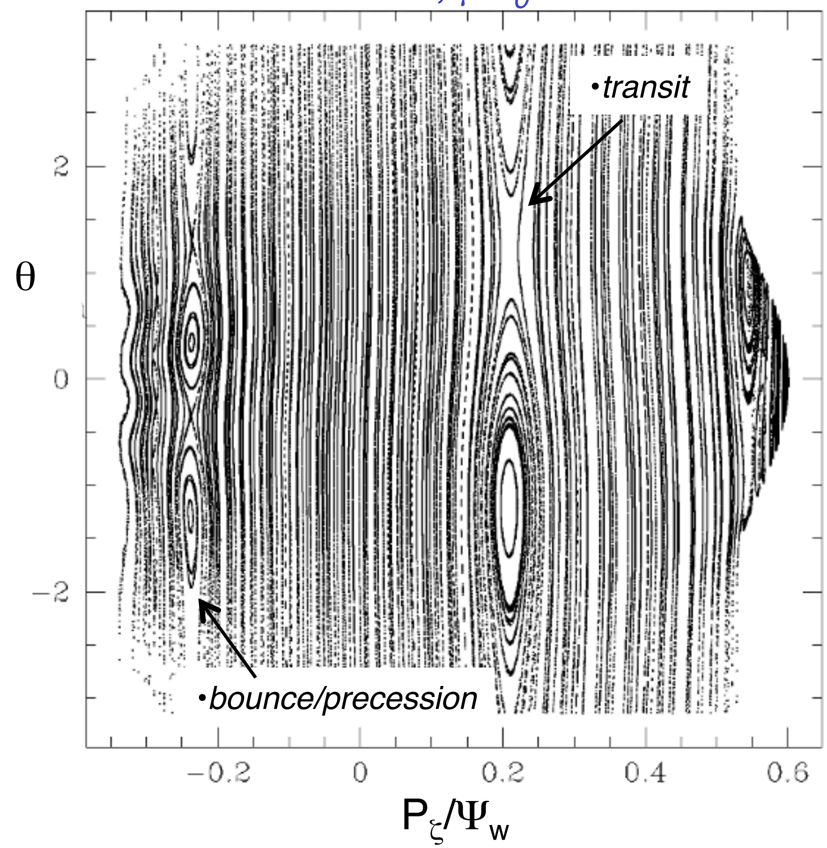

> Possible tool to compute β_{res} more accurately

Summary and conclusions

- The kink-like mode stability properties and dynamics in NSTX plasmas are analyzed in this study.
- The NRK and fishbone stability diagram from the experimental data indicates that the kink-like modes appear mostly for $q_{\min} < 1.5$
- The long lived NRK modes tend to be unstable at higher fast ion β.
- The bursting modes have an increased real-frequency as the minimum q and ratio of fast ion pressure and total plasma pressure increase.
- Experimental results will provide the basis for the validation and benchmark of numerical studies of the kink-like instabilities.

Future work: Comparison of the database with simulations of kink-like modes on NSTX

- This experimental characterization of kink-like modes for different NBI scenarios provides reference for simulations of kink-like instabilities in NSTX plasmas for a variety of scenarios, particularly for different fast ion properties.
- Simulations with the GTC code[16] will be used to assess the kinetic effects of thermal and fast ions on the instabilities and identify regimes for which kink/fishbone activity is minimized or suppressed.
- Experimental plasma parameters from the database including the thermal equilibrium and measured fast ion profiles can be implemented and used as initial conditions.

This work is partly supported by US-DoE contract DE-AC02- 09CH11466

NSTX equilibrium and preliminary kink simulations in GTC fluid limit

- Experimental equilibrium from shot # 124379 has been implemented in GTC.
- q profile is modified to test the numerical capabilities. Simulations in fluid limit is being carried out for benchmark purposes.

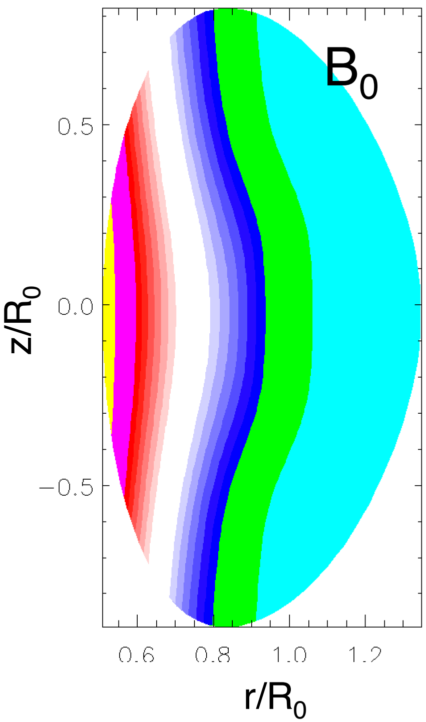

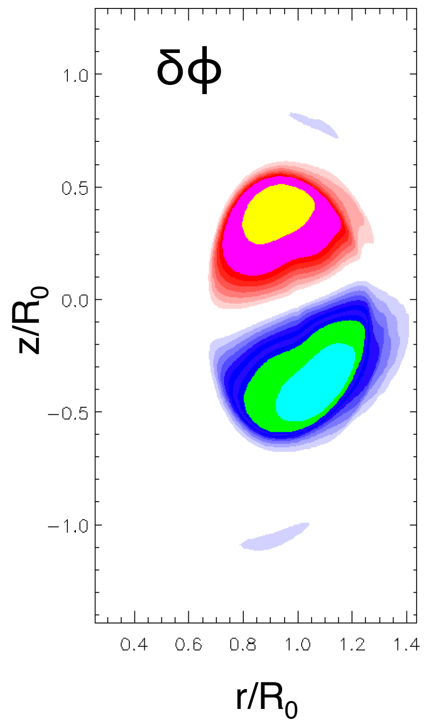

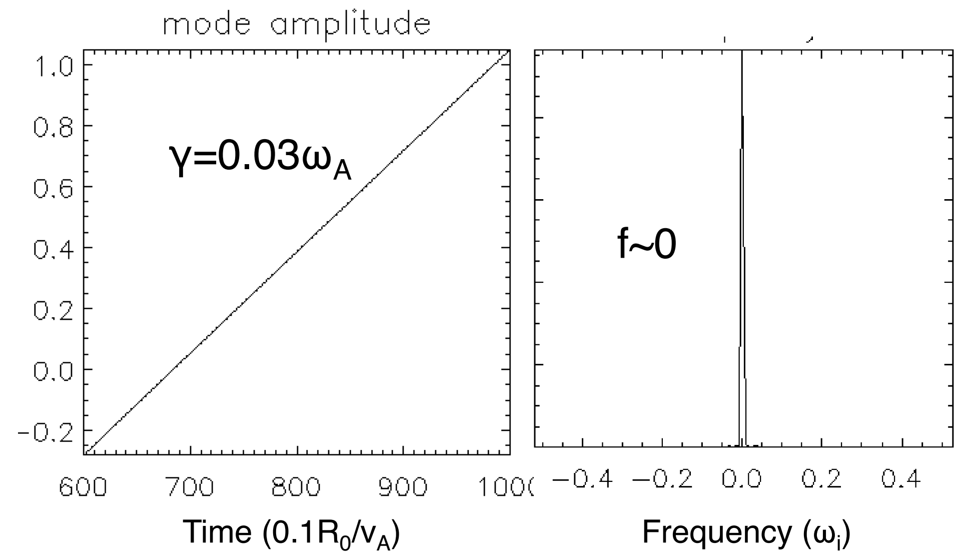

n_e=9.34×10^{19} m^{-3}

T_e=879.96 eV *(artificially increased to 2.3keV to match experimental total beta in fluid limit simulations)*

R_0=101.83 cm

B_0=4536 G

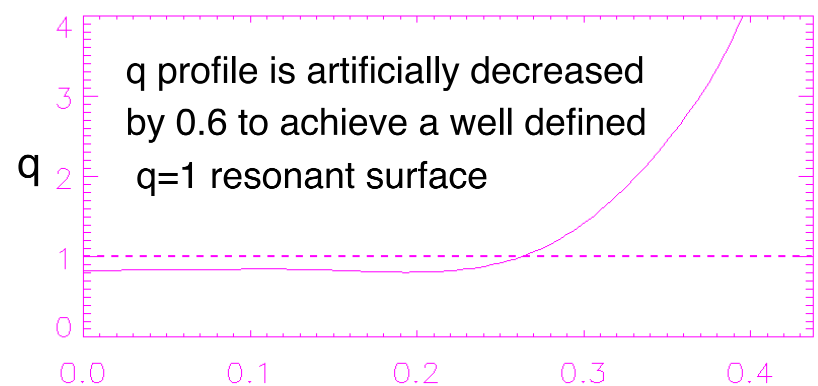

Reference

[1] M. Ono, et. al., Nucl. Fusion 40, 557 (2000).
[2] F. Levinton and H. Yuh, Review of Scientific Instruments 79, 10F522 (2008).
[3] M. Podesta, et. al., Nucl. Fusion 51, 063035 (2011).
[4] L. Chen, R. B. White and M. N. Rosenbluth, Phys. Rev. Lett. 52, 1122-1125 (1984). [5] E. Frederickson, L. Chen, and R. B. White, Nucl. Fusion 43, 1258-1264 (2003).
[6] M. N. Bussac, et. al., Phys. Rev. Lett. 35, 1638 (1975).
[7] J. Breslau, et. al., Nucl. Fusion 51, 063027 (2011).
[8] T. Hender, et. al., Nucl. Fusion 47, S128 (2007).
[9] A. Odblom, et. al., Phys. Plasmas 9, 155 (2002).
[10] F. Wang, et. al., Phys. Plasmas 20, 102506 (2013).
[11] A. Mishchenko and A. Zocco, Phys. Plasmas 19, 122104 (2012). [12] R. Hastie, et. al., Phys. Fluids 30, 1756 (1987).
[13] R. Bell, et. al., Phys. Plasmas 17, 082507 (2010).
[14] M. Podesta, et. al., Phys. Plasmas 16, 056104 (2009).
[15] A. Brizard, Phys. Plasmas 18, 022508 (2011).
[16] J. McClenaghan, et. al., submitted, *http://phoenix.ps.uci.edu/zlin/bib/bib.htm* (2014).